

Microwave surface-impedance measurements of the electronic state and dissipation of magnetic vortices in superconducting LiFeAs single crystals

T. Okada,^{1,3} H. Takahashi,^{1,3} Y. Imai,^{1,3} K. Kitagawa,^{2,3} K. Matsubayashi,^{2,3} Y. Uwatoko,^{2,3} and A. Maeda^{1,3}

¹*Department of Basic Science, The University of Tokyo, Meguro, Tokyo 153-8902, Japan*

²*Institute for Solid State Physics, The University of Tokyo, Kashiwa, Chiba 277-8581, Japan*

³*Transformative Research Project on Iron Pnictides (TRIP), JST, Chiyoda, Tokyo 102-0075, Japan*

(Received 29 October 2011; revised manuscript received 14 June 2012; published 14 August 2012)

LiFeAs is one of the iron-based superconductors that has multiple gaps with a possible sign reversal. To clarify how those characteristics affect the energy dissipation of magnetic vortices, we investigated the microwave surface impedance of LiFeAs single crystals under finite magnetic fields. The flux-flow resistivity enhanced rapidly at low magnetic fields, which is similar to the case of MgB₂. This is probably a consequence of the multiple-gap nature and the gap anisotropy. This suggests that the sign reversal is not important for the flux flow, even for multiple-gap superconductors. As for the electronic state, the vortex core of LiFeAs turned out to be “moderately clean.” Furthermore, the mean free path inside the vortex core was much shorter than that outside, and was close to the core radius. These results strongly suggest that a process specific to the core boundary is important for a scattering mechanism inside the vortex core.

DOI: [10.1103/PhysRevB.86.064516](https://doi.org/10.1103/PhysRevB.86.064516)

PACS number(s): 74.70.Xa, 74.25.Wx, 72.15.Lh, 74.25.nn

Ever since the discovery of LaFeAsO_{1-x}F_x with $T_c = 26$ K,¹ iron-based superconductors (SCs) have attracted a lot of attention. Because multiple bands contribute to the Fermi surfaces and the magnetic phase exists in the vicinity of the superconductive phase in the phase diagram, it is expected that the mechanism of superconductivity of iron-based SCs is different from that of conventional SCs. New possibilities of superconducting gap structures based on the interband scattering, such as s^\pm -wave^{2,3} and s^{++} -wave,^{4,5} were suggested theoretically. Experimentally, although this issue is under debate,⁶ phase-sensitive experiments⁷⁻⁹ suggested that s^\pm -state was realized in some materials of iron-based SCs. The electronic structure and dynamic properties of vortices in such a novel class of SCs are of great interest.

As for conventional SCs, the quasiparticle (QP) excitation inside the vortex core has quantized energy levels with the spacing $\Delta E \sim \Delta^2/E_F \equiv \hbar\omega_0$, where Δ and E_F are the size of the superconducting gap and the Fermi energy, respectively, and with the width $\delta E \sim \hbar/\tau_{\text{core}}$, where τ_{core} is the relaxation time of QPs inside the vortex core.^{10,11} The ratio of these two energy scales, $\Delta E/\delta E \sim \omega_0\tau_{\text{core}}$, is a barometer of the quantum nature of the electronic state inside the vortex core. Depending on this number, we have the following three regimes: (i) the dirty regime ($\omega_0\tau_{\text{core}} \ll 1$), (ii) the moderately clean regime ($\omega_0\tau_{\text{core}} \sim 1$), and (iii) the superclean regime ($\omega_0\tau_{\text{core}} \gg 1$). It should be noted that $\omega_0\tau_{\text{core}}$ is connected to the viscous drag coefficient, η , and the carrier density, n , as $\omega_0\tau_{\text{core}} = \eta/n\pi\hbar$.¹²

According to Kopnin and Volovik (KV),¹³ the flux-flow resistivity of a single-gap SC, ρ_f , behaves in magnetic fields, B , as

$$\frac{\rho_f}{\rho_n} \approx \frac{\Delta_0^2}{\langle \Delta^2(\theta) \rangle_{\text{FS}}} \frac{B}{B_{c2}} \quad (B \ll B_{c2}), \quad (1)$$

where ρ_n , B_{c2} , Δ_0 , and $\langle \Delta^2(\theta) \rangle_{\text{FS}}$ are the resistivity in the normal state, the upper critical field, the maximum size of the superconducting gap, and the angular average of the superconducting gap on the Fermi surface, respectively. This

suggests that (i) ρ_f in the low- B region increases linearly with B , and (ii) the gradient, $\alpha \equiv \Delta_0^2/\langle \Delta^2(\theta) \rangle_{\text{FS}}$, becomes larger than unity when $\Delta(\theta)$ depends on the angle θ . In fact, for an isotropic gap case, the Bardeen-Stephen (BS) theory¹⁴ obviously obeys Eq. (1). On the other hand, in the nodal and modulated gap case, an enhancement with $\alpha > 1$ in the low- B region has also been observed experimentally.¹⁵⁻¹⁸ This also suggests that the so-called “Volovik effect” (in which the effect of the Doppler shift on QPs disperses as a result of the circulating supercurrents) is not important for the flux flow in the low- B region, although it succeeded to explain the B dependences of the specific heat and the thermal conductivity. As for the two-band s^{++} -wave SCs, such as MgB₂ and Y₂C₃, a rapid enhancement of $\rho_f(B)$ was observed.^{19,20} This can be interpreted as a superposition of two linear B dependences corresponding to two bands.²¹ Thus, $\rho_f(B)$ reflects the superconducting gap structure and its symmetry. Therefore, it is very interesting how the flux-flow resistivity of the novel class of SCs behaves as a function of B . However, the flux flow of such novel SCs has not been investigated at all either theoretically or experimentally. Thus, it is a great challenge to investigate the flux flow of iron-based SCs.

We focus on a 111 material, LiFeAs. This material has the highest T_c of 18 K (Ref. 22) among stoichiometric iron-based SCs, and single crystals with high quality [residual resistivity ratio (RRR) ~ 50] can be obtained. The band calculation²³ suggested that Fermi surfaces consist of two holelike and two electronlike pockets around Γ points and M points, respectively. Nodeless multiple superconducting gaps were observed by angle-resolved photoemission spectroscopy (ARPES)^{24,25} and a specific-heat measurement,²⁶ and superfluid-density data^{27,28} showed that LiFeAs has a nodeless multiple-gap structure. In addition to the phase-sensitive experiment in Li-111,⁹ the electrical conductivity, σ_1 ,²⁸ estimated from the microwave surface impedance and the nuclear spin-lattice relaxation rate, $1/T_1$,²⁹ do not show the so-called “coherence peak” below T_c . These strongly suggest that LiFeAs has an

s^\pm -wave gap structure. Therefore, we can agree with the standpoint that Li-111 is an s^\pm -SC.

In this paper, we report on the surface impedance of LiFeAs single crystals under finite magnetic fields, and we discuss the electronic state inside the vortex core. It was clarified that the field dependence of the flux flow of an s^\pm -state is similar to that of an s^{++} -state, and that the vortex core of LiFeAs is moderately clean. The estimated mean free path of QPs inside the vortex core was found to be much shorter than that outside, and was comparable to the core radius. This suggests that the mechanism characteristic of the core boundary plays an important role in the dissipative process inside the vortex core.

LiFeAs single crystals were grown by a self-flux method²⁸ and were cleaved under an Ar atmosphere in a glove box. The typical sample size was $0.5 \times 0.5 \times 0.2 \text{ mm}^3$, and the demagnetization coefficient estimated under ellipsoidal approximation was about 0.58. These were of very high quality, with $\text{RRR} \equiv \rho_{\text{dc}}(300 \text{ K})/\rho_{\text{dc}}(T_c) \sim 45$, and the dc resistivity behaved as $\rho_{\text{dc}}(T > T_c) = \rho_0 + AT^2$ ($\rho_0 \approx 30 \mu\Omega \text{ cm}$, $A \approx 6.5 \times 10^{-2} \mu\Omega \text{ cm/K}^2$), which is typical of the Fermi liquid dominated by the electron-electron scattering. Since LiFeAs is moisture-/atmosphere-sensitive, samples were covered with Apiezon N grease during the measurement. We confirmed that Apiezon N grease does not affect the results discussed below in a different comparative experiment.

The microwave surface impedance was measured by using a cavity perturbation technique³⁰ with a cylindrical oxygen-free Cu cavity resonator operated at $\omega/2\pi \sim 19 \text{ GHz}$ in the TE_{011} mode. The Q factor was $Q \gtrsim 6 \times 10^4$, and the filling factor of the samples was about 6×10^{-6} . Both the external magnetic field up to 8 T and the microwave magnetic field were applied parallel to the c axis. Therefore, we investigated the in-plane vortex motion.

The surface impedance, $Z_s = R_s - iX_s$ (R_s and X_s are the surface resistance and the surface reactance, respectively), is related to the resonant frequencies, $\omega_s/2\pi$ and $\omega_b/2\pi$, and the Q factors, Q_s and Q_b , as $R_s = G(1/2Q_s - 1/2Q_b)$, $X_s = G(1 - \omega_s/\omega_b) + C$, where the subscripts s and b represent the values measured with and without the sample, respectively, and G, C are constants determined by the size and the shapes of the sample and the resonator. The magnitudes of R_s and X_s are obtained by assuming the Hagen-Rubens relation $R_s = X_s = \sqrt{\mu_0\omega\rho_{\text{dc}}/2}$ in the normal state.

Z_s in the mixed state was calculated by Coffey and Clem (CC).³¹ Their calculation is based on the equation of motion of the massless vortex, $\eta\dot{\mathbf{u}} + \kappa\mathbf{u} = \Phi_0\mathbf{J} \times \hat{\mathbf{z}} + \mathbf{f}(t)$, where \mathbf{u} is the displacement of a vortex, κ is the pinning force constant, $\Phi_0 = h/2e = 2.07 \times 10^{-15} \text{ Wb}$ is the flux quantum, \mathbf{J} is the transport current density, and $\hat{\mathbf{z}}$ is the unit vector in the applied field direction. The effect of thermal fluctuations and the Hall effect are effectively included in random force, $\mathbf{f}(t)$, and η , respectively, for circulating microwave currents. At low temperature, the flux-creep contribution becomes negligibly small and the CC model leads to the relation

$$Z_s = -i\mu_0\omega\sqrt{\frac{\lambda_L^2 + \frac{1}{\mu_0\omega}\rho_f(1 - i\frac{\omega_{\text{cr}}}{\omega})^{-1}}{1 + is}}, \quad (2)$$

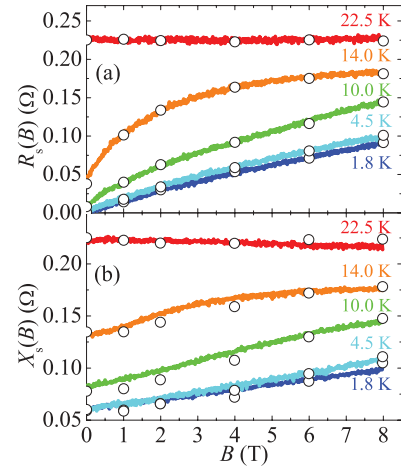


FIG. 1. (Color online) The magnetic field dependence of (a) the surface resistance, R_s , and (b) the surface reactance, X_s , of a LiFeAs single crystal at 19 GHz up to 8 T at various temperatures. The curves and the open circles represent the data taken in the swept magnetic field (fixed temperatures) and in the swept temperature (fixed magnetic fields), respectively.

where λ_L is the London penetration depth and $\omega_{\text{cr}}/2\pi$ is the crossover frequency characterizing the crossover between reactive and resistive response, and $s = \mu_0\omega\lambda_L^2/\rho_n$, which represents the normal-fluid contribution. One can assume that s is negligible at low temperatures. Consequently, we obtain ω_{cr} and ρ_f from experimental data of R_s and X_s by solving Eq. (2).

Figure 1 shows the magnetic field dependence of Z_s at various temperatures. Good agreement between temperature-swept data and magnetic-field-swept data indicates that the magnetic field penetrates uniformly in the sample. With increasing magnetic field, both R_s and X_s increase monotonically. In particular, R_s shows a convex upward behavior. We determine the zero-field superconducting transition temperature, $T_c^{\text{onset}} = 17 \text{ K}$, from the temperature dependence of X_s in zero magnetic field, which is in good agreement with the previously reported number in the same batch.²⁸

The obtained crossover frequency of $\omega_{\text{cr}}/2\pi \approx 3 \text{ GHz}$ is larger than that of conventional SCs ($\approx 100 \text{ MHz}$) (Ref. 32) but smaller than that of copper-oxide SCs by one order of magnitude.^{33,34} A similar value of ω_{cr} has been reported in a 1111-type polycrystal ($\approx 6 \text{ GHz}$).³⁵ The tendency that ω_{cr} becomes small at high temperatures is consistent with a general description that the thermal fluctuation decreases the pinning force.

Figure 2 shows the normalized flux-flow resistivity as a function of the normalized magnetic field. The flux-flow resistivity of LiFeAs single crystals increased linearly with B , suggesting that the KV model is appropriate even for this material. As for the gradient, α of LiFeAs is larger than that of the conventional s -wave case ($\alpha = 1$) and smaller than that of the d -wave (with lines of node) case ($\alpha \approx 2$). This enhancement of $\rho_f(B)$ may be derived from one or both of two origins. The first possible origin is based on the multiple-band nature. As for the two-band SCs, such as MgB_2 and Y_2C_3 , the superposition of two linear dependences corresponding to two

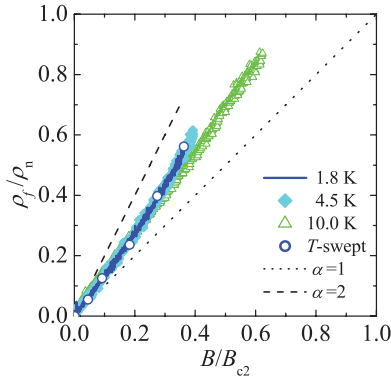


FIG. 2. (Color online) The magnetic field dependence of the flux-flow resistivity $\rho_f(B)$ of the LiFeAs single crystal at several temperatures. The blue open circle is $\rho_f(B)$ at $T = 1.8$ K obtained from temperature-swept data. The gradients, α , expected in d -wave (with lines of node) SCs ($\alpha \approx 2$) and in conventional s -wave SCs ($\alpha = 1$) are also shown as dashed and dotted lines, respectively.

bands causes the flux-flow resistivity to enhance rapidly at low B .^{19,20} We can speculate that the five-band nature of LiFeAs probably induces a similar tendency. The second possibility is based on the gap anisotropy. Recent ARPES data suggest that some of the superconducting gaps have obvious fourfold angle dependences.²⁵ Based on the KV model, this angle dependence of the superconducting gap will make the gradient of $\rho_f(B)$ larger than unity ($\alpha > 1$). In any case, the magnetic field dependence of ρ_f of LiFeAs is very similar to that of MgB₂, implying that the s^\pm -wave SC behaves essentially similarly to the s^{++} -wave SC so far as the flux-flow is concerned. The insensitivity of the flux flow to the sign change for single-gap SCs has already been known for single-gap SCs; although the anisotropic s -wave SC and the d -wave SC differ from each other in the sign change of the order parameter, ρ_f of both SCs exhibits a B -linear dependence with $\alpha > 1$.^{16–18} Our present result shows that the insensitivity shown in the flux flow is applicable also for multiple-gap SCs.

Figure 3 shows the temperature dependence of the viscous drag coefficient, $\eta = \Phi_0 B / \rho_f$. η is well fitted by the ex-

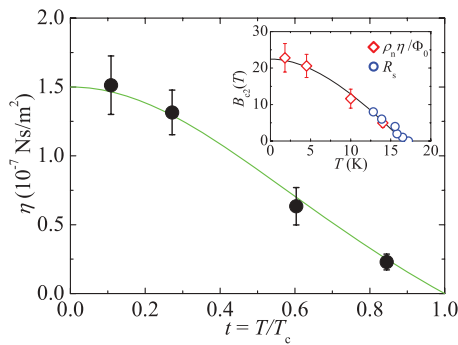


FIG. 3. (Color online) The temperature dependence of the viscous drag coefficient, $\eta = \Phi_0 B / \rho_f$. The green solid line is the expectation in the GL theory, $\eta(t) = \eta(0)(1 - t^2)/(1 + t^2)$. The inset shows the temperature dependence of B_{c2} obtained from T_c^{onset} from the temperature dependence of R_s (blue open circle), and that calculated from ρ_n and η (red open diamond). The solid line is to guide the eye.

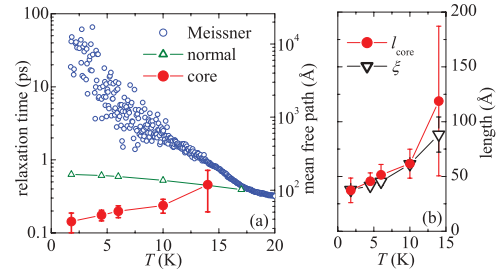


FIG. 4. (Color online) (a) Temperature dependences of relaxation times and mean free paths of QPs in several states. Symbols are those outside the vortex core (blue open circle), in the normal state (green open triangle), and inside the vortex core (red solid circle), respectively. (b) Temperature dependences of the mfp inside the vortex core (red circle) and the coherence length calculated from $B_{c2}(T)$ (black triangle).

pected temperature dependence in the Ginzburg-Landau (GL) theory, $\eta(T) = \eta(0)[1 - (T/T_c)^2]/[1 + (T/T_c)^2]$. From the fitting, we obtain $\eta(0) = (1.5 \pm 0.2) \times 10^{-7}$ Ns/m². We can estimate the upper critical field as $B_{c2}(T) = \rho_n(T)\eta(T)/\Phi_0$, where $\rho_n(T) = \rho_0 + AT^2$ is extrapolated as $\rho_{dc}(T > T_c)$ in the temperature regions $T < T_c$. The result is shown in the inset. We obtain $B_{c2}(0) = 22 \pm 4$ T. Similar numbers were reported previously in the same material.^{36–41} Considering the moisture-/atmosphere-sensitive nature of LiFeAs and the difference of RRR values among these crystals, we consider that it is within the range of individual differences.

In Fig. 4, we discuss the relaxation time and the mean free path (mfp) of QPs inside the vortex core. Since $\lambda_L^{-2}(T) = \mu_0 e^2 n_s(T) / m^*$, using the value $m^*/m_0 = 5.2–6.3$ (m_0 is the free-electron mass)^{42,43} and $\lambda_L(0) = X_s(0)/\mu_0 \omega \sim 390$ nm, we estimate the carrier density $n \approx n_s(0) = (9.6–11.7) \times 10^{20}$ cm⁻³, which gives $\omega_0 \tau_{\text{core}} = 0.4–0.5$. This shows that the vortex core of LiFeAs is in the moderately clean regime. Furthermore, by using the number $-\hbar\omega_0/2 = -0.9$ meV observed in a recent scanning tunneling microscopy/spectroscopy (STM/STS) study,⁴⁴ we obtain the relaxation time of QPs inside the vortex core, $\tau_{\text{core}}(1.8 \text{ K}) \approx 0.15$ ps. This value is quite different from that outside (≈ 10 ps),²⁸ and is even smaller than that in the normal state (≈ 0.6 ps). These results are shown in Fig. 4(a). From the relaxation time, we found the mfp of QPs inside the vortex core to be $l_{\text{core}} = v_F \tau_{\text{core}} \approx 40$ Å, where $v_F \approx 2.6 \times 10^4$ m/s is the Fermi velocity, which is estimated from STM/STS⁴⁴ and ARPES data.^{24,25} Again, this value is much shorter than that outside the core, l_{Meissner} . In particular, as shown in Fig. 4(b), l_{core} is comparable to the coherence length, ξ , estimated from B_{c2} . We checked the repeatability in another single crystal of LiFeAs, and the results were consistent with those described above. In addition, we performed the same measurements in LiFe(As,P) single crystals, which was at most 3% P-substituted, and we obtained similar results.

The short mfp of QPs inside the vortex core was also observed in many copper-oxide SCs, such as YBa₂Cu₃O_{7-x}, Bi₂Sr₂CaCu₂O_y, and La_{2-x}Sr_xCuO₄.^{45–47} In these cuprates, the mfp inside the vortex core is also much shorter than that outside and rather close to the core radius, $l_M \gg l_{\text{core}} \sim \xi$.

Similarly, in Y_2C_3 ,²⁰ which is one of the two-gap SCs with an isotropic s -wave, the mfp inside the vortex core is limited to the coherence length, $l_{\text{core}} \lesssim \xi$. It is surprising that a similar tendency was observed among many different SCs with different gap structures, pairing mechanisms, and electronic structures. Since the relation $l_{\text{core}} \sim \xi$ was obtained, one can consider that a scattering process which is specific to the core boundary contributes to the additional dissipation in the vortex core, as was originally considered by Nozières and Vinen for clean SCs.⁴⁸ Indeed, Eschrig *et al.*⁴⁹ discussed that the Andreev reflection at the core boundary is crucial even in the flux flow of moderately clean SCs, and they showed theoretically that there is extra energy dissipation at low frequencies because of the presence of a collective mode. However, it is not yet clear whether this mechanism can explain the large dissipation observed in our experiments quantitatively at present. A systematic study of the frequency dependence of the in-core dissipation will clarify the validity of Eschrig's model. On the other hand, according to Tinkham⁵⁰ and Nozières-Vinen-Warren,^{48,51} the relaxation time $\tau_{\text{gap}} = \hbar/\Delta_0$, which is characteristic of the moving vortex, has been considered. For LiFeAs, $\tau_{\text{gap}} = 0.2$ ps is comparable to the obtained τ_{core} . To clarify the validity of these models, studies of the gap-size dependence of τ_{core} are needed.

In conclusion, we investigated the microwave surface impedance of LiFeAs single crystals under finite magnetic fields. The magnetic field dependence of the flux-flow resistivity of a new class of superconductors having multiple gaps with a possible sign reversal became clear. The flux-flow resistivity increased linearly with the magnetic field, as was suggested by Kopnin-Volovik. In particular, the gradient at low fields was larger (smaller) than that of conventional s -wave superconductors (d -wave superconductors with lines of node). This is probably a consequence of the multiple-gap nature and/or the gap anisotropy. This also suggests that the flux-flow resistivity is insensitive to the sign reversal of the order parameter on different Fermi surfaces. As for the electronic state, the vortex core of LiFeAs was estimated to be moderately clean. The mean free path of quasiparticles inside the vortex core was much shorter than that outside, and was comparable to the core radius, suggesting the importance of the Andreev reflection at the core boundary. Such a tendency was observed also in many other superconductors, and systematic studies will clarify the dissipative mechanism inside the vortex core.

We thank Tetsuo Hanaguri for showing us many unpublished data and also for fruitful discussions. We also thank Masashi Takigawa for providing us with LiFeAs single crystals, and Yusuke Kato for valuable comments.

¹Y. Kamihara *et al.*, *J. Am. Chem. Soc.* **130**, 3296 (2008).

²I. I. Mazin, D. J. Singh, M. D. Johannes, and M. H. Du, *Phys. Rev. Lett.* **101**, 057003 (2008).

³K. Kuroki, S. Onari, R. Arita, H. Usui, Y. Tanaka, H. Kontani, and H. Aoki, *Phys. Rev. Lett.* **101**, 087004 (2008).

⁴S. Onari and H. Kontani, *Phys. Rev. Lett.* **103**, 177001 (2009).

⁵Y. Yanagi, Y. Yamakawa, and Y. Ono, *Phys. Rev. B* **81**, 054518 (2010).

⁶P. J. Hirschfeld, M. M. Korshunov, and I. I. Mazin, *Rep. Prog. Phys.* **74**, 124508 (2011).

⁷T. Hanaguri *et al.*, *Science* **328**, 474 (2010).

⁸C. T. Chen *et al.*, *Nat. Phys.* **6**, 260 (2010).

⁹T. Hanaguri *et al.* (unpublished).

¹⁰C. Caroli *et al.*, *Phys. Lett.* **9**, 307 (1964).

¹¹H. F. Hess, R. B. Robinson, R. C. Dynes, J. M. Valles, and J. V. Waszczak, *Phys. Rev. Lett.* **62**, 214 (1989).

¹²G. Blatter *et al.*, *Rev. Mod. Phys.* **66**, 1125 (1994).

¹³N. B. Kopnin and G. E. Volovik, *Phys. Rev. Lett.* **79**, 1377 (1997).

¹⁴J. Bardeen and M. J. Stephen, *Phys. Rev.* **140**, A1197 (1965).

¹⁵S. Kambe, A. D. Huxley, P. Rodiere, and J. Flouquet, *Phys. Rev. Lett.* **83**, 1842 (1999).

¹⁶Y. Tsuchiya, K. Iwaya, K. Kinoshita, T. Hanaguri, H. Kitano, A. Maeda, K. Shibata, T. Nishizaki, and N. Kobayashi, *Phys. Rev. B* **63**, 184517 (2001).

¹⁷Y. Matsuda, A. Shibata, K. Izawa, H. Ikuta, M. Hasegawa, and Y. Kato, *Phys. Rev. B* **66**, 014527 (2002).

¹⁸K. Takaki, A. Koizumi, T. Hanaguri, M. Nohara, H. Takagi, K. Kitazawa, Y. Kato, Y. Tsuchiya, H. Kitano, and A. Maeda, *Phys. Rev. B* **66**, 184511 (2002).

¹⁹A. Shibata, M. Matsumoto, K. Izawa, Y. Matsuda, S. Lee, and S. Tajima, *Phys. Rev. B* **68**, 060501(R) (2003).

²⁰S. Akutagawa, T. Ohashi, H. Kitano, A. Maeda, J. Goryo, H. Matsukawa, and J. Akimitsu, *J. Phys. Soc. Jpn.* **77**, 064701 (2008).

²¹J. Goryo and H. Matsukawa, *Physica B* **359**, 533 (2005).

²²J. H. Tapp, Z. Tang, B. Lv, K. Sasmal, B. Lorenz, P. C. W. Chu, and A. M. Guloy, *Phys. Rev. B* **78**, 060505R (2008).

²³D. J. Singh, *Phys. Rev. B* **78**, 094511 (2008).

²⁴S. V. Borisenko *et al.*, *Phys. Rev. Lett.* **105**, 067002 (2010).

²⁵K. Umezawa *et al.*, *Phys. Rev. Lett.* **108**, 037002 (2012).

²⁶F. Wei, F. Chen, K. Sasmal, B. Lv, Z. J. Tang, Y. Y. Xue, A. M. Guloy, and C. W. Chu, *Phys. Rev. B* **81**, 134527 (2010).

²⁷H. Kim, M. A. Tanatar, Y. J. Song, Y. S. Kwon, and R. Prozorov, *Phys. Rev. B* **83**, 100502 (2011).

²⁸Y. Imai *et al.*, *J. Phys. Soc. Jpn.* **80**, 013704 (2011).

²⁹Z. Li *et al.*, *J. Phys. Soc. Jpn.* **79**, 083702 (2010).

³⁰A. Maeda *et al.*, *J. Phys.: Condens. Matter* **17**, R143 (2005).

³¹M. W. Coffey and J. R. Clem, *Phys. Rev. Lett.* **67**, 386 (1991).

³²J. I. Gittleman and B. Rosenblum, *Phys. Rev. Lett.* **16**, 734 (1966).

³³M. Golosovsky, M. Tsindlekht, H. Chayet, and D. Davidov, *Phys. Rev. B* **50**, 470 (1994).

³⁴S. Revenaz, D. E. Oates, D. Labbe-Lavigne, G. Dresselhaus, and M. S. Dresselhaus, *Phys. Rev. B* **50**, 1178 (1994).

³⁵A. Narduzzo *et al.*, *Phys. Rev. B* **78**, 012507 (2008).

³⁶N. Kurita *et al.*, *J. Phys. Soc. Jpn.* **80**, 013706 (2011).

³⁷J. L. Zhang, L. Jiao, F. F. Balakirev, X. C. Wang, C. Q. Jin, and H. Q. Yuan, *Phys. Rev. B* **83**, 174506 (2011).

³⁸K. Cho, H. Kim, M. A. Tanatar, Y. J. Song, Y. S. Kwon, W. A. Coniglio, C. C. Agosta, A. Gurevich, and R. Prozorov, *Phys. Rev. B* **83**, 060502(R) (2011).

- ³⁹M. A. Tanatar, J.-Ph. Reid, S. Ren de Cotret, N. Doiron-Leyraud, F. Lalibert, E. Hassinger, J. Chang, H. Kim, K. Cho, Yoo Jang Song, Yong Seung Kwon, R. Prozorov, and Louis Taillefer, *Phys. Rev. B* **84**, 054507 (2011).
- ⁴⁰O. Heyer, T. Lorenz, V. B. Zabolotnyy, D. V. Evtushinsky, S. V. Borisenko, I. Morozov, L. Harnagea, S. Wurmehl, C. Hess, and B. Büchner, *Phys. Rev. B* **84**, 064512 (2011).
- ⁴¹Y. J. Song *et al.*, *Appl. Phys. Lett.* **96**, 212508 (2010).
- ⁴²C. Putzke *et al.*, *Phys. Rev. Lett.* **108**, 047002 (2012).
- ⁴³S. Kasahara, K. Hashimoto, H. Ikeda, T. Terashima, Y. Matsuda, and T. Shibauchi, *Phys. Rev. B* **85**, 060503 (2012).
- ⁴⁴T. Hanaguri, K. Kitagawa, K. Matsubayashi, Y. Mazaki, Y. Uwatoko, and H. Takagi, *Phys. Rev. B* **85**, 214505 (2012).
- ⁴⁵A. Maeda *et al.*, *J. Phys. Soc. Jpn.* **76**, 094708 (2007).
- ⁴⁶A. Maeda *et al.*, *Physica C* **362**, 127 (2001).
- ⁴⁷A. Maeda, T. Umetsu, and H. Kitano, *Physica C* **460**, 1202 (2007).
- ⁴⁸P. Nozières and W. F. Vinen, *Philos. Mag.* **14**, 667 (1966).
- ⁴⁹M. Eschrig, J. A. Sauls, and D. Rainer, *Phys. Rev. B* **60**, 10447 (1999).
- ⁵⁰M. Tinkham, *Phys. Rev. Lett.* **13**, 804 (1964).
- ⁵¹W. F. Vinen and A. C. Warren, *Proc. Phys. Soc.* **91**, 409 (1967).